

Multi-scale Kinetic Modeling and Experimental Investigation of Syngas Production from Coal Gasification in Updraft Gasifiers

Michele Corbetta,[†] Andrea Bassani,[†] Flavio Manenti,^{*,†} Carlo Pirola,[‡] Enrico Maggio,[§] Alberto Pettinau,[§] Paolo Deiana,^{||} Sauro Pierucci,[†] and Eliseo Ranzi[†]

[†]Dipartimento di Chimica, Materiali e Ingegneria Chimica (CMIC) “Giulio Natta”, Politecnico di Milano, Piazza Leonardo da Vinci, 32, 20133 Milano, Italy

[‡]Dipartimento di Chimica, Università degli Studi di Milano, Via Golgi, 19, 20133 Milano, Italy

[§]Sotacarbo SpA, Grande Miniera di Serbariu, 09013 Carbonia, Italy

^{||}Energy and Plants, ENEA, Casaccia Research Center SP 81, Via Anguillarese, 301, 00123 Santa Maria di Galeria, Roma, Italy

Received: March 31, 2015

Revised: May 17, 2015

1. INTRODUCTION

The gasification of coal, biomass, and refuse-derived fuel (RDF) is an attractive way to efficiently exploit the energetic content of solid fuels in a greener fashion. Beyond direct applications in the power generation field,¹ the syngas produced from this kind of process could provide an interesting platform for the production of fuels and chemicals with a lower environmental footprint.² Actually, several gas-to-liquid technologies are available for the production of hydrocarbons, e.g., Fischer–Tropsch fuels³ and oxygenated chemicals, e.g., methanol and dimethyl ether.^{4–6} For these applications, it is crucial to focus the attention on the quality of the syngas produced, mostly in terms of the H₂/CO ratio.⁷ In fact, the downstream catalytic processes typically need to be fed with a syngas with a proper composition, usually in the range of H₂/CO \approx 1–2.⁸ For this reason, it is of the utmost importance to be able to predict the performance of a gasifier, not only in terms of the overall efficiency but also in relation to the chemical composition of the syngas produced.

The remarkable interest in coal and/or biomass gasifiers is well-testified by the massive recent literature. Mostly, these papers discuss experimental work on the performances of different solid feeds, equipment, and operating conditions.^{9–15} For instance, Galindo et al.⁹ analyzed the temperature effect on the quality of syngas in a two-stage downdraft gasifier, measuring tar and particle content at different operating conditions. Prabowo et al.¹⁶ assessed the feasibility of CO₂ as an alternative gasifying agent with a lab-scale downdraft gasifier, comparing experimental results to those obtained from pyrolysis in an inert atmosphere. Patel et al.¹⁰ studied the

effect of the particle size on the gasification efficiency in a pilot-scale downdraft gasifier.

On the other side, several papers propose mathematical models to better understand the complex phenomena occurring in gasifiers, with an interest toward the design, simulation, optimization, and process analysis of the gasification processes. These papers mainly refer to mathematical models based on thermodynamic equilibrium and/or strongly simplified kinetics.^{17–27} It is clear that thermodynamic models are very useful tools for preliminary comparison and for process assessment on the influence of major process parameters.²⁸ They have the advantage of being independent of reactor design, assuming zero-dimensional perfectly mixed reactors at uniform temperatures. Gasification reaction rates are supposed to be fast enough to reach the equilibrium state, but they are not able to give information on reaction intermediates and formation of tar components.^{20,22–25,27} Following this approach, Bassyouni et al.¹⁹ simulated palm waste gasification using commercial simulation packages with a conversion reactor for the pyrolysis zone and equilibrium and Gibbs reactors for the combustion of char and volatiles. The same approach has been applied by Keche et al.²¹ for the simulation of biomass in downdraft gasifiers and by Tapasvi et al.²⁶ for the simulation of torrefied biomass gasification.

Finally, other papers discuss mathematical models of the gasifier with particular attention to computational fluid

dynamics (CFD) simulations with pyrolysis and secondary gas-phase reactions, often very simplified. Generally, they refer to entrained-flow or fluidized-bed reactors.^{29–32} Zhong et al.³¹ recently investigated pitch-water slurry gasification in downdraft and entrained-flow gasifiers with large attention to CFD with only a few reactions to characterize the secondary gas-phase chemistry. Masmoudi et al.³² developed a thermokinetic two-dimensional (2D) steady-state model for the simulation of a downdraft biomass gasifier. They found that particle size plays a major role on hydrogen and carbon monoxide yields and distributions. The modeling work of Ismail et al.²⁹ deals with an updraft gasifier. They adopted only one lumped component to characterize the biomass, and there is only one secondary gas-phase reaction describing the pyrolysis of the lumped tar species. The work of Vascellari et al.³⁰ constitutes a very complete example of a mathematical model of an entrained-flow gasifier. Coal devolatilization is modeled using an empirical two-step model. Char gasification is modeled using a n th-order intrinsic kinetics model. The eddy dissipation concept (EDC) accounts for the turbulence–chemistry interaction in combination with the a kinetic mechanism, including 22 species in the gas phase. Generally, all of these models are computationally very expensive, thus requiring, in contrast, a greater simplification in the chemistry of the process.

The novelty of the proposed approach consists in a greater chemical detail of the kinetics of solid fuel pyrolysis and the devolatilization process as well as the kinetics of char gasification and secondary gas-phase reactions. Multi-step kinetic models for the pyrolysis of solid fuels were embedded within a particle model, along with gas–solid reactions and secondary gas-phase reactions.^{33,34} Lastly, the solution of this multi-phase and multi-component problem at the reactor scale requires careful numerical attention, and specifically conceived numerical methods have been adopted. The chemical evolution of the overall gasification system is predicted with a mechanistic model; hence, it is possible to predict the unit performance even with greater detail with respect to the available experimental data. The mathematical model of the updraft gasifier is used to perform a careful sensitivity analysis to key operating parameters, such as oxygen/fuel and steam/fuel ratios, inlet gas temperature, and composition. Some preliminary comparisons of model predictions to literature experimental data are also proposed to further validate the model reliability.³⁵ Moreover, experimental data from the Sotacarbo pilot plant, located in Sardinia, Italy,³⁶ constitute a further test case for this multi-scale kinetic and reactor model. Namely, these data allow for analysis and assessment of the important catalytic role of ash in the low-temperature steam gasification of coal.

It seems well-established that the reactivity of higher rank bituminous charcoals with steam below 700–800 °C is lower than that of lignite or lower rank coals. Timpe and co-workers³⁷ experimentally found that this low reactivity can be significantly enhanced by adding ~5 wt % potassium. Furthermore, the difficulties in properly defining the ash catalytic effect on charcoal gasification was also discussed and highlighted by several authors.^{37,38} Similarly, experimental studies comparing the reactivity of lignite, deashed lignite, and deashed lignite impregnated with different loads of catalytically active elements demonstrated that sodium and calcium can significantly increase the char reactivity, while magnesium and iron have an opposite effect.^{39,40}

In this context, the model represents a very important support to the pilot-scale experimental activities. As a matter of facts, it allows for the design and optimization of the experimental campaigns in the pilot unit by predicting plant performance in several operating conditions (to reduce the number of experimental tests). On the other hand, experimental data could be used to refine the model and to further improve its accuracy.

This present work is structured as follows. Section 2 provides information about the experimental facilities of the Sotacarbo pilot plant, while section 3 reports the comprehensive mathematical model, focusing the attention on both the kinetic schemes and the particle and the reactor models. Finally, section 4 compares the results of the simulations of updraft coal gasifiers to two independent sets of experimental data, emphasizing the ash catalytic effect. A sensitivity analysis to guide the selection of optimal process operating conditions is also reported.

2. SOTACARBO PILOT PLANT

The Sotacarbo pilot plant is based on a fixed-bed updraft gasifier (Figure 1), derived from a properly simplified



Figure 1. Sotacarbo pilot gasifier.

Wellmann–Galusha gasification technology, equipped with a very flexible syngas treatment system for both power generation and hydrogen production with CO₂ capture. The gasifier is a cylinder characterized by an internal diameter of 300 mm and a total height of 2000 mm, with the external wall covered by refractory material and a metallic grate that supports the fuel bed. A cone below the grate allows for both ash discharge and the feeding of air and steam, typical gasification agents. Coal, with a particle size between 5 and 15 mm, is charged in a proper hopper and drowned out into the gasifier. It constitutes the fuel bed, with a typical height of about 1000–1200 mm,

where coal drying, devolatilization, pyrolysis, gasification, and combustion processes take place, at pressures of 0.11–0.14 MPa. As the coal particles move downward, they are heated by the hot gases that flow upward.

The gasification agents, eventually preheated up to 250 °C, are introduced below the fuel grate, so that they are preheated by cooling the bottom ashes and react with the fuel bed in the combustion and gasification zones. Dry ashes are periodically discharged through the grate, whereas raw syngas leaves the reactor at the top. Temperature profiles inside the reactor are measured through a probe, located near the reactor vertical axis and equipped with a series of 11 K-type thermocouples (with a measure range up to 1200 °C) and through another series of 34 thermocouples located near the grate and the wall of the reactor.

The startup of the gasifier is carried out using a series of three ceramic lamps, located near the bottom of the fuel bed, which preheat the fuel in an inert atmosphere (nitrogen flow). Wood pellets are usually mixed with a small amount of paraffinic material to promote the successive bed ignition as soon as air is injected into the reactor after the preheating phase.

The gasification unit has been tested for about 2500 h (since 2008) with several kinds of coal (lignite, bituminous, and sub-bituminous coals) and biomass (wood pellets). Table 1 summarizes average plant performance with the most

Table 1. Typical Gasification Conditions and Performance

	South African	Usibelli	Hungarian	Sulcis	wood chips
Operating Parameters					
fuel consumption (kg/h)	8.0	24.0	11.0	9.2	12.0
air mass flow (kg/h)	36.8	57.6	20.0	39.2	11.3
steam mass flow (kg/h)	3.7	3.7	2.0	2.5	0.0
Raw Syngas Composition (Molar Fractions, Dry Basis)					
CO	0.1807	0.2368	0.1943	0.1583	0.2207
CO ₂	0.0947	0.0771	0.0864	0.0948	0.0797
H ₂	0.1889	0.1779	0.1042	0.1200	0.3342
N ₂	0.5128	0.4729	0.5759	0.5606	0.3418
CH ₄	0.0151	0.0173	0.0162	0.0236	0.0119
H ₂ S	0.0003	0.0002	0.0049	0.0119	0.0000
COS	0.0001	0.0001	0.0008	0.0019	0.0000
O ₂	0.0074	0.0176	0.0099	0.0233	0.0117
other (C ₂ H ₆ and C ₃ H ₈)	0.0000	0.0001	0.0074	0.0054	0.0000
Raw Syngas Properties (Dry Basis)					
mass flow (kg/h)	46.83	79.67	24.19	48.91	23.31
volume flow (Nm ³ /h)	42.90	72.90	20.34	41.55	25.48
LHV (MJ/kg)	4.50	5.14	3.55	3.59	7.49
specific heat (kJ/kg K)	1.23	1.23	1.12	1.14	1.47
outlet pressure (MPa)	0.14	0.14	0.14	0.14	0.14
Main Gasifier Performance Indicators					
peak temperature (°C)	1034	1066	900	950	730
cold gas efficiency (%)	96.93	96.13	98.97	90.60	84.33
gasifier yield (Nm ³ /kg)	5.36	3.04	1.85	4.52	2.12
SGR-GL (kg m ⁻² h ⁻¹)	113.2	339.5	155.6	130.1	169.8

representative fuels tested in the Sotacarbo platform: a South African high-ash bituminous coal, a high-sulfur sub-bituminous coal from Sulcis coal mine (southwest Sardinia, Italy), two lignites from Alaska and Hungary, and stone pine (*Pinus pinea*) wood chips.

This table also shows the main gasifier performance indicators. In particular, the gasifier yield is defined as the ratio between the volume flow of produced syngas (Nm³/h) and the mass flow of primary fuel (kg/h), and the specific gasification rate (SGR, expressed in kg m⁻² h⁻¹) is defined as the amount of gasified fuel (kg/h) divided by the area (m²) of the horizontal section of the fuel bed.

More experimental campaigns with new fuels will be performed soon with the support of the simulation model, with the goal to collect new data and to further improve the model itself.

3. MATHEMATICAL MODEL OF SOLID FUEL GASIFIERS

The complexity of the detailed description of solid fuel gasification processes is mainly due to the coupling of the kinetics and transport phenomena occurring in this multi-component, multi-phase, and multi-scale system. From a chemical point of view, gasification takes place from the multi-phase interactions between a solid fuel and a gaseous stream (composed of steam, oxygen, or carbon dioxide), resulting in a progressive degradation of the solid matrix with a partial oxidation of char and released volatiles. At the particle scale, the solid fuel initially requires being heated and dried until devolatilization and pyrolysis can occur. This stage is endothermic, and the required heat is conveniently provided by the exothermic partial oxidation reactions of char and volatiles. At the reactor scale, a countercurrent configuration allows for the sustainable autothermal operation of the gasifier. Consequently, it is convenient to start with the analysis of kinetics and, only after, to focus the attention on the balance equations at the particle and reactor scales.

3.1. Kinetic Models. As schematically outlined in Figure 2, the chemical evolution of the system during the gasification process requires a kinetic description at three different levels: (1) solid fuel devolatilization and pyrolysis, (2) residual solid (char) gasification and combustion with steam, CO₂, and oxygen, and (3) secondary gas-phase reactions of released volatiles.

The heated solid fuel is transformed in a metaplastic phase, progressively releasing light gases and tar species. The residual solid is composed of ash and char, with a residual content of volatiles trapped within the porous matrix, and it is ready to interact with the gas phase.

Coal devolatilization and pyrolysis are described with a multi-step kinetic model, extensively validated by Sommariva et al.⁴¹ Different coals are characterized as a mixture of reference lumped species, COAL1, COAL2, and COAL3, representative of different coal ranks, for which first-order devolatilization kinetics are provided. This model was further extended and improved by Maffei et al.^{53–55}

After the first devolatilization step, the residual char is more available to gas–solid endothermic gasification and/or exothermic combustion reactions with steam and oxygen, with a relevant production of carbon monoxide and hydrogen. Three different char species (CHARH, CHAR, and CHARG) are considered to better describe their different reactivity and possible annealing effects.⁴²

Dependent upon the temperature and residence time, secondary gas-phase reactions are responsible for the successive pyrolysis and oxidation of gases and heavy tar species, thus increasing syngas production. A detailed kinetic model is used for this purpose.⁴³ Several POLIMI_1411 kinetic schemes that involve more than 450 species and about 15 000 reactions are available on the website <http://creckmodeling.chem.polimi.it/>.

3.2. Particle and Reactor Models. To model and simulate the updraft gasifier, it is necessary to properly describe both kinetic and transport processes. This leads to the solution of a multi-scale dynamic

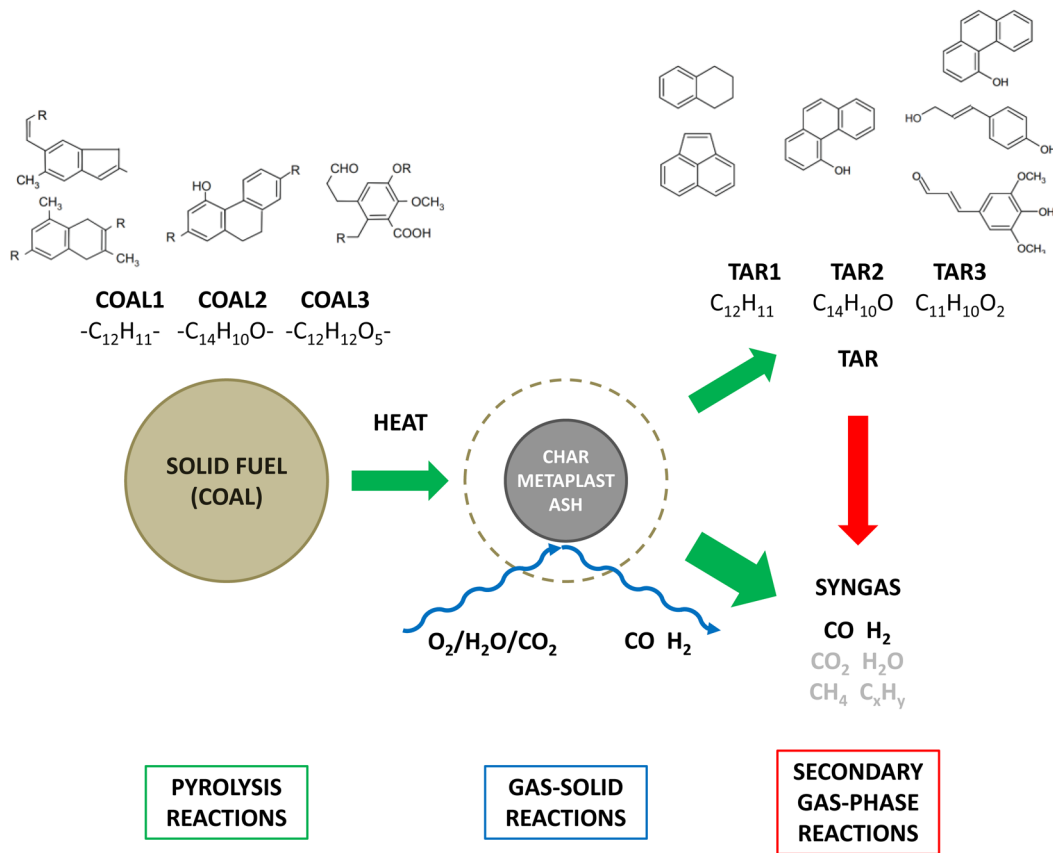


Figure 2. Solid fuel devolatilization, gasification, and partial oxidation, with pyrolysis in green, gas–solid reactions in blue, and secondary gas-phase reactions in red.

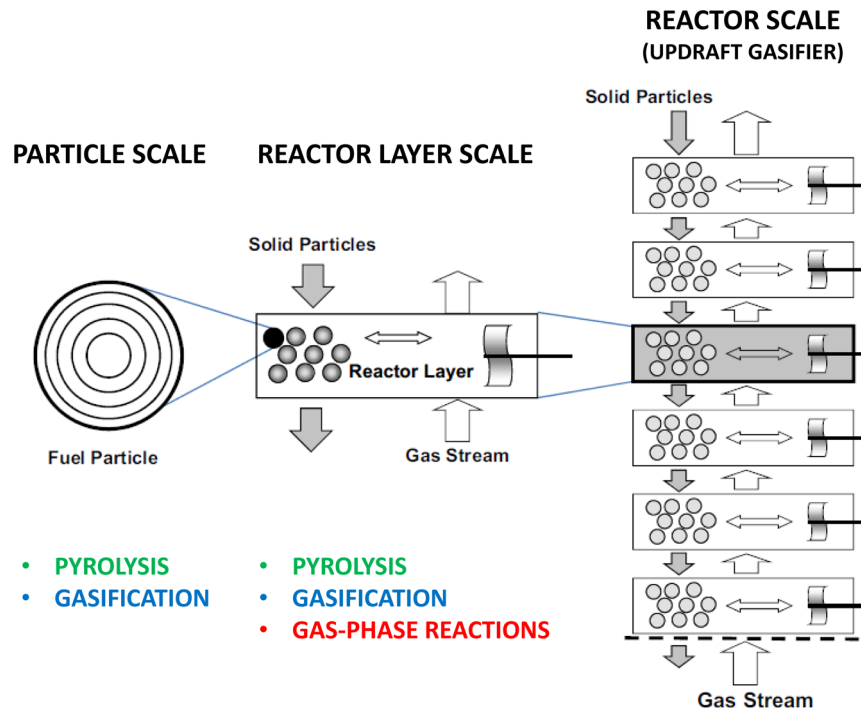


Figure 3. Representation of the multi-scale structure of the mathematical model for the description of updraft gasifiers.

system, spanning from the description of kinetic and transport aspects at the particle scale up to the description of mass and energy transfer as well as secondary reactions at the reactor scale.⁴⁴ The system is intrinsically multi-phase, because of the combined presence of gas,

liquid, and solid phases, which exchange mass and energy, increasing in this way the overall complexity of this system.⁴⁵ The structure of the gasifier is outlined in Figure 3, where the multi-scale nature of this problem is highlighted. At the particle scale, fuel pellets are described

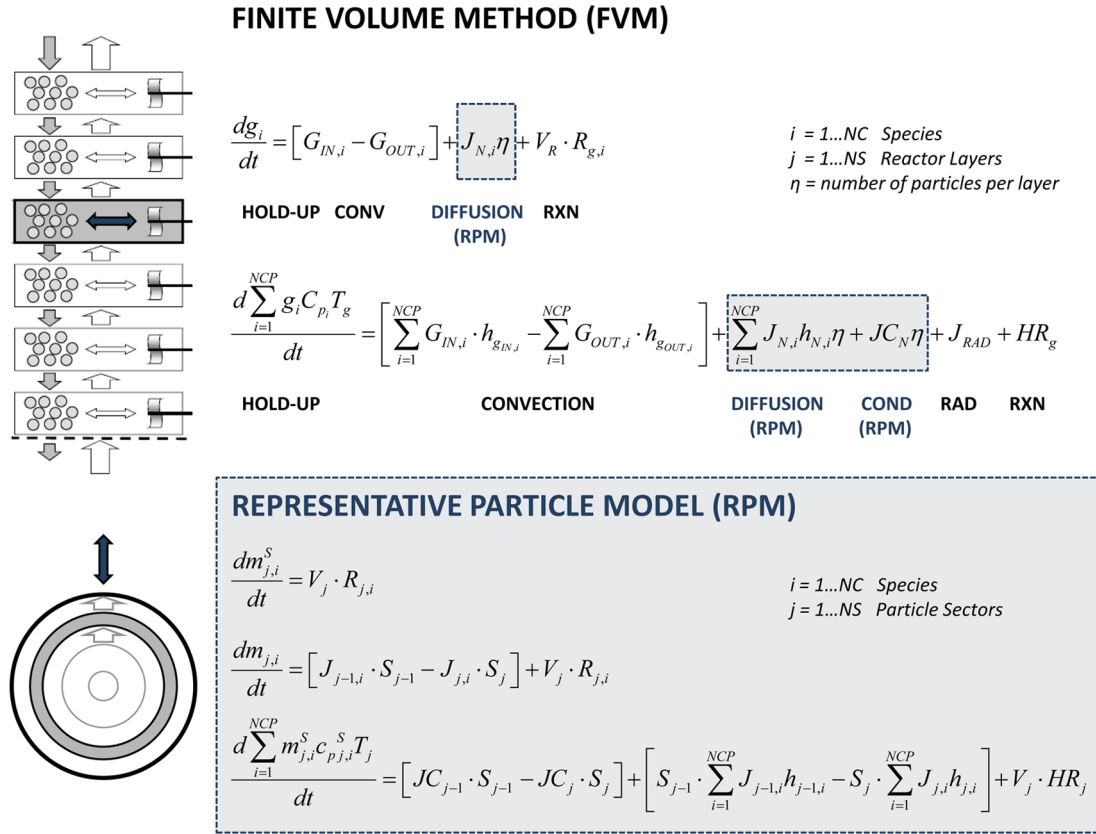


Figure 4. Mass and energy balance equations at the reactor scale (FVM) and the particle scale (RPM).

with a one-dimensional (1D) model using an equivalent spherical diameter, to reduce the computational burden. The dynamic evolution of the intraparticle temperature and species composition profiles is obtained. The elementary reactor layer allows us to account for the coupling between fuel particles and a perfectly mixed surrounding gas phase, where secondary reactions occur. Finally, at the reactor scale, several elementary reactor layers are considered. Different networks of interconnected reactor layers permit reproduction of several reactor configurations. The comprehensive mathematical model of the gasifiers implements a finite volume method (FVM) with a representative particle model (RPM), with two levels of spatial discretization.

The first level is the particle radial discretization, depending upon the number of particle sectors, while the second level is the reactor axial discretization, depending upon the number of reactor layers.

Thus, the countercurrent fixed-bed (updraft) gasifier is modeled through a cascade of elementary reactor layers. The solid fuel is fed from the top of the reactor where it encounters the rising gas stream, fed from the bottom of the tower. During the residence time within the gasifier, particles are progressively dried, pyrolyzed, and gasified, leading to the residual char withdrawn from the bottom and a gas stream rich in hydrogen and carbon dioxide exiting from the top.

Figure 4 reports the mass and energy balances at the particle scale as well as the mass and energy balances at the elementary reactor layer scale. The dimension of the resulting differential algebraic equation (DAE) system easily overcomes several thousands of equations, and it is dictated by the number of lumped species in the solid phase (15–30), the number of sectors at the particle scale (5–10), the number of species in the gas phase (100–200), and finally, the number of reactor layers (10–20).

The mathematical complexity of the system is mainly due to the stiffness nature of the kinetics and demands for efficient and robust solvers.^{46,47} The DAE system is solved with the BzzMath numerical library available on the website <http://super.chem.polimi.it/>. A more

complete description of this set of equations and the related Jacobian matrix sparsity pattern is provided elsewhere.⁴⁴

4. MODEL PREDICTIONS AND COMPARISONS TO EXPERIMENTAL DATA

To prove the reliability of the model of the updraft gasifier, two independent sets of experimental data will be analyzed.

4.1. Operating Conditions of the Two Sets of Experiments. The operating conditions and the main input parameters for model simulations are summarized in Table 2.

Table 2. Input Parameters for the Simulation of the Two Set of Experiments

parameter	Grieco and Baldi ³⁵	Pettinau et al. ³⁶
coal C/H/O (wt %)	80.1:5.1:15.8	87.9:5.0:7.1
ash (wt %)	9	15
moisture (wt %)	17.4	8
particle diameter (cm)	2.54	2.75
inlet gas temperature (K)	373	373
peak temperature (K)	~1650	~1200
equivalence ratio	0.176	0.122
air/coal ratio	1.81	1.40
steam/coal ratio (STC)	0.30	1.03
SGR (kg m ⁻² h ⁻¹)	342.7	99.08

These conditions refer to the lab-scale gasifier reported in ref 35 and a sample of the experimental data obtained in the Sotacarbo pilot plant. Before comparison of model predictions to experimental data, it is convenient to analyze and assess some model features particularly with respect to the spatial

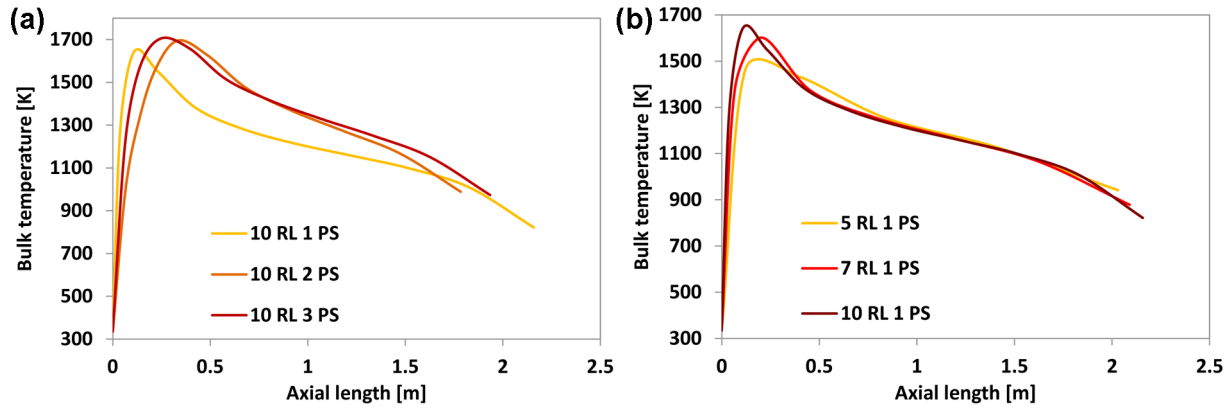


Figure 5. Effect of spatial discretization on temperature profiles: (a) effect of the number of PSs and (b) effect of the number of RLs.

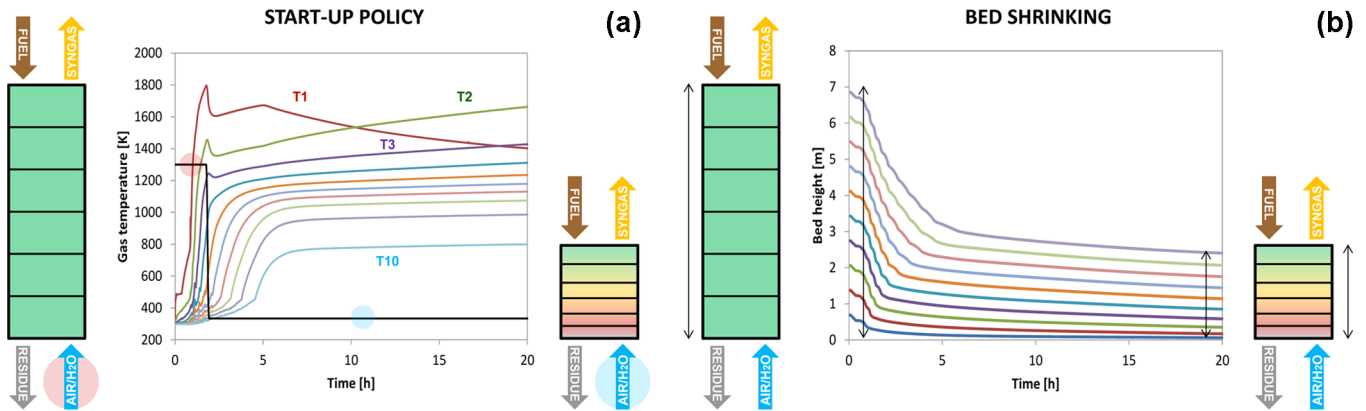


Figure 6. (a) Gas-phase temperature dynamic profiles during the startup and (b) RL height evolution during the startup procedure.

discretization and the dynamic behavior to reach the steady-state conditions, referring to the Grieco and Baldi gasifier.³⁵

4.2. Sensitivity Analysis to Particle and Reactor Discretization. The sensitivity of the mathematical model toward spatial discretization is performed by changing both particle radial discretization [number of isovolumetric particle sectors (PSs)] and reactor axial discretization [number of elementary reactor layers (RLs)]. Figure 5 shows the sensitivity of the temperature profiles with respect to PS (Figure 5a) and RL (Figure 5b). This sensitivity analysis highlights the importance to use more than 5–7 RLs and 2 particle discretizations. This is a compromise between simulation accuracy and computational time.

The effect of particle discretization is very pronounced, because of the large diameter of coal particles (2.54 cm). A thermally thick regime occurs within the particles,³³ which requires us to account for thermal resistances. When the number of PSs is increased, the combustion zone moves toward the top of the gasifier because of the thermal penetration time necessary to heat thick particles. The presence of several PSs results in a wider combustion region, because of the progressive heating and reaction of the internal sectors. On the other hand, the number of RLs slightly impacts the resolution of the combustion zone and the corresponding temperature hot spot.

4.3. Startup Procedure. To further highlight the complexity of this problem, two different peculiarities of the updraft gasifier are analyzed. The first peculiarity is strictly related to the autothermal behavior of the updraft gasifier, where thermal feedback is realized between exothermic partial oxidation and combustion reactions and endothermic drying, pyrolysis, and

gasification reactions. This fact forces on applying a suitable startup policy to reach the desired “hot” gasification conditions, avoiding the “cold” steady solution. This is true from both an operational and a numerical point of view. In the industrial practice, a duct burner is usually adopted to preheat inlet gas to start up the gasifier, providing the required heat to the endothermic pyrolysis and gasification reactions. Once the char and volatile partial oxidation and combustion take place, the system self-maintains the hot conditions and becomes autothermal and the auxiliary burner is shut down.⁴⁸ Simulation conditions mimic this startup procedure. The inlet gas temperature is initially set to 1300 K until combustion occurs in the first layer ($T > 1800$ K) and, only then, is lowered to 300 K. Figure 6a shows the time histories of temperature profiles of the different reactor layers. The startup procedure lasts about 5600 s, after which the gas inlet temperature is gradually reduced to 300 K. The steady-state condition inside the gasifier is reached only after more than 20 h, with a slight progressive shift of the combustion front toward the upper layers. It is important to observe that the complete gasification reached at the bottom of the gasifier determines a $\sim 90\%$ reduction of the mass, because of the presence of less than 10% ash.

For this reason, it is necessary to account for significant morphological changes in the effective dimension of the reactor layers, because of the shrinking of the fuel particles during the gasification process, i.e., along the gasifier. Figure 6b shows the height evolution of the solid bed. Only a moderate bed shrinking occurs during the startup phase, where the combustion reactions mostly take place in the gas phase. The system reaches the steady-state condition only after the

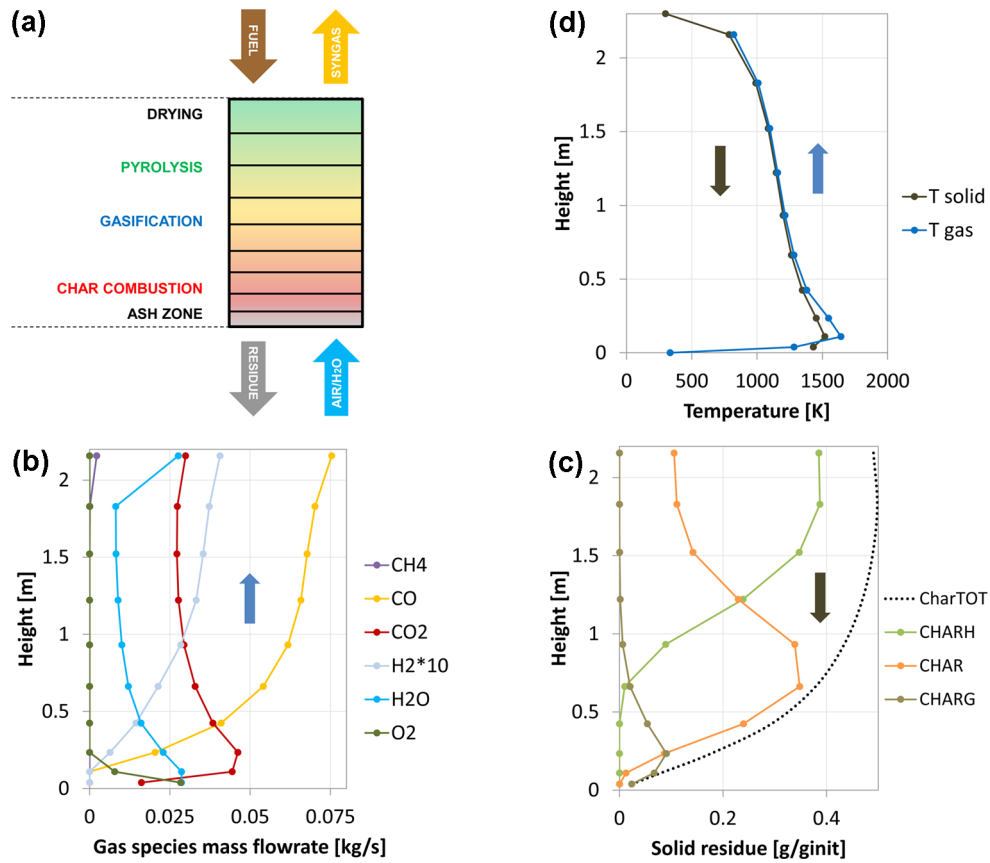


Figure 7. (a) Schematic of chemical phenomena occurring within the updraft gasifier, (b) mass flow rate of key gas components, (c) residual solid composition, and (d) thermal profiles along the gasifier axial length (Grieco and Baldi case study³⁵).

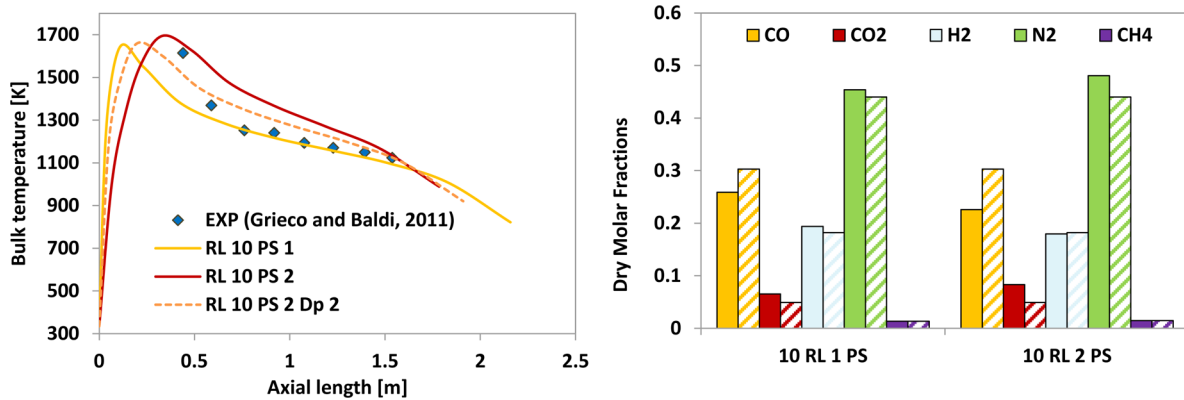


Figure 8. Comparisons of experimental data (dashed bars) to model predictions (solid bars).

completion of coal devolatilization and char gasification, which is the time-limiting step of the overall process.

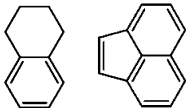
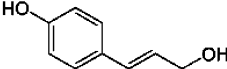
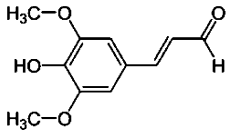
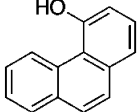
4.4. Comparison to Experimental Data of the Lab-Scale Gasifier. The comprehensive mathematical model provides detailed information on chemical and physical phenomena occurring inside the gasifier. Figure 7 shows the axial temperature and composition profiles of both the solid and gas phases.

Figure 7a shows the schematic of the chemical phenomena involved in the countercurrent gasification process. Moving from the top downward, solid particles are dried, pyrolyzed, gasified, and burnt. The temperatures at the bottom of the gasifier overcome 1500–1600 K. In the bottom layer, the hot residual char and ash heat the rising oxidizer stream, completing

the solid-phase combustion. Further oxidation reactions in the gas phase are responsible for the relevant production of CO₂ and the temperature peak that overcomes the solid temperature. At these high temperatures, the endothermic gasification reactions of both steam ($\text{CHAR} + \text{H}_2\text{O} \rightarrow \text{CO} + \text{H}_2$) and CO₂ ($\text{CHAR} + \text{CO}_2 \rightarrow 2\text{CO}$) contribute to CO and H₂ production.

The cascade of chemical steps is reflected in the axial evolution of the mass flow rate of the key species in both the gas and solid phases. Carbon dioxide is initially produced in the bottom reactor layers, and it is then consumed by the gasification reactions, while it is slightly produced in the upper reactor zone because of secondary gas-phase oxidation reactions. A significant steam increase is observed in the top reactor layer, mainly because of the drying of wet coal. Methane

Table 3. Detailed Syngas Composition, Including Gas and Tar Species and Lumped Components

Species	Model			Exp data	
	wt %	mol %	mol dry %	mol dry %	
N ₂	46.001	39.569	45.407	44.0	
H ₂	1.413	16.885	19.376	18.2	
H ₂ O	9.612	12.857	-	-	
CO	26.220	22.557	25.885	30.3	
CO ₂	10.393	5.691	6.530	4.9	
CH ₄	0.772	1.159	1.330	1.6	
C ₃ H ₆	0.380	0.218	0.250	n/a	
C ₂ H ₄	0.201	0.173	0.198	n/a	
CH ₂ O	0.076	0.061	0.070	n/a	
CH ₃ OH	0.082	0.062	0.071	n/a	
BENZENE	0.402	0.124	0.142	n/a	
TOLUENE	0.558	0.146	0.167	n/a	
FUEL1		0.097	0.018	0.021	n/a
COUMARYL		0.341	0.055	0.063	n/a
SINAPOYL ALDEHYDE		0.354	0.041	0.047	n/a
FENAOH		3.095	0.384	0.441	n/a

is produced in the upper part of the gasifier because of coal devolatilization and secondary gas-phase pyrolysis reactions. These reactions are also responsible for the final inflection of the CO profile. Figure 7d shows the char formation and successive transformations along the reactor. The char presence in the first layer of the gasifier indicates the occurrence of a relevant coal devolatilization. Finally, it is important to observe that CHARG is the ultimate product of the pyrolytic char transformations, and it is the rate-determining step for the overall gasification process and the major product responsible for carbon content in residual ash.

The experimental data reported by Grieco and Baldi³⁵ allow for further validation of the coal gasifier model. The leucite sub-bituminous coal (C/H/O/N/S = 78.1:5:14.4:1:1.2) is considered in the following study. A total of 10 reactor layers are assumed, while 1 and 2 particle sectors are considered in two different simulations. Comparisons between experimental data and model predictions, both in terms of bulk temperature profiles and syngas composition, are shown in Figure 8.

As already observed, the hot spot location is more correctly predicted by the simulation performed with 2 particle sectors (PS 2), while the 1 particle sector simulation (PS 1) shows a slightly lower temperature peak, too close to the gas inlet zone, but agrees better with the experimental temperature profile in the upper zone of the gasifier. The predicted syngas composition, together with the char content in the residual ashes, indicates that the PS 1 simulation improves the gasification efficiency with respect to the PS 2 simulation. This fact is also confirmed by the average lower temperatures in PS 1 simulation, because of the higher extent of the endothermic gasification process. Both of these simulations reasonably fit experimental data in terms of both temperature and product distribution. A better agreement, mainly in terms of temperature profiles, is obtained using a slightly lower equivalent spherical diameter (2 cm, instead of 2.54 cm), as shown by the dotted line in Figure 8. For the sake of completeness, the detailed composition of syngas, predicted by the model, is reported in Table 3.

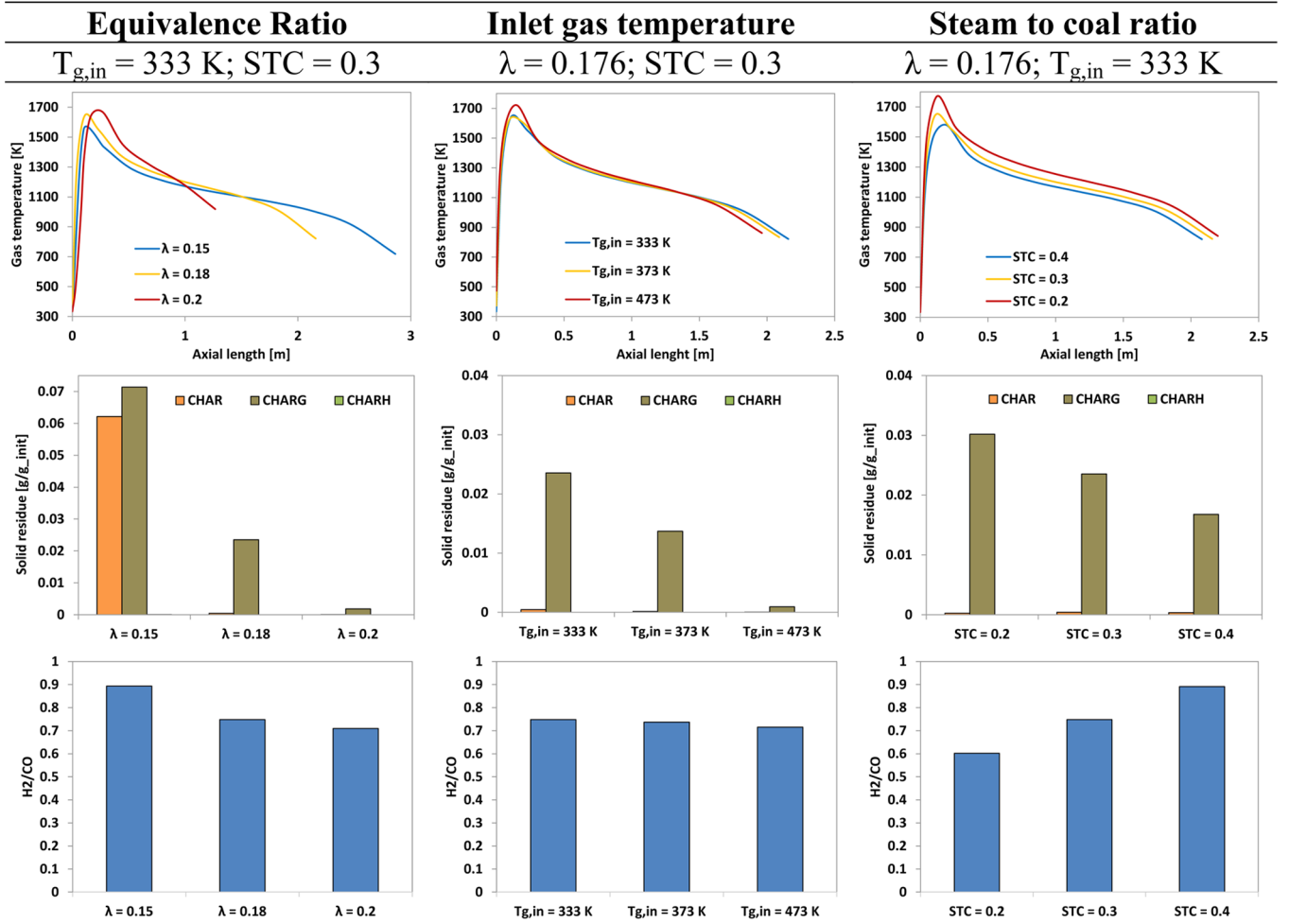


Figure 9. Sensitivity analysis of the equivalence ratio, inlet gas temperature, and STC on temperature profiles, gas species, and solid residue.

Even though the composition of minor species was not experimentally measured, the accuracy of the POLIMI kinetic model in predicting single-ring aromatic and oxygenated tar compounds has been recently proven by Stark et al.⁴⁹

To exploit the possibilities of the proposed model better, a parametric study of some key operating parameters, such as inlet gas composition and temperature, is proposed here. Model predictions always refer to the previously analyzed base case.³⁵ As already mentioned, the complexity of this simulation problem demands computing times of several hours. For this reason, moving from the steady-state solution of the base case, stepwise input changes are imposed on the investigated operating conditions. The new steady-state solution is thus reached in a more effective way.

Figure 9 and Table 4 show the effect of the equivalence ratio (ER = $1/\lambda$), the inlet gas temperature, and the mass steam/carbon ratio (STC = steam flow/coal flow) on gasifier performances, in terms of temperature profiles, syngas composition, residual solid, and gasification efficiency.

λ is defined as the ratio between actual and stoichiometric air

$$\lambda = \frac{\dot{m}_{\text{air}}}{\dot{m}_{\text{air,stoich}}} \quad (1)$$

where $\dot{m}_{\text{air,stoich}}$ is calculated on the basis of the elemental coal composition $C_iH_jO_k$.

$$\dot{m}_{\text{air,stoich}} = \frac{MW_{\text{air}} \dot{m}_{\text{coal}}}{MW_{\text{coal}} x_{\text{O}_2, \text{air}}} \left(i + \frac{j}{4} - \frac{k}{2} \right) \quad (2)$$

In eq 2, \dot{m}_{coal} and $\dot{m}_{\text{air,stoich}}$ are the coal mass flow rate and the corresponding stoichiometric air. MW_{coal} and MW_{air} are the molecular weights of coal and air, respectively.

Cold gas efficiency (CGE) is the energy input over the potential energy output and is defined here as the ratio between the chemical power of raw syngas over the chemical power associated with coal.

$$\text{CGE} = \frac{\text{syngas power}}{\text{fuel power}} = \frac{\dot{m}_{\text{syngas}} \text{HHV}_{\text{syngas}}}{\dot{m}_{\text{fuel}} \text{HHV}_{\text{fuel}}} \quad (3)$$

The higher heating value (HHV) of coal is obtained with the following formula,^{50,51} leading to a value of 28.7 MJ/kg for the Grieco and Baldi coal:

$$\text{HHV}_{\text{fuel}} = 34.2C + 132.2H + 12.3S - 12.0(O + N) - 1.5\text{ash} \quad (\text{MJ/kg}) \quad (4)$$

In eq 4, the elemental coal composition is given in mass fractions on a dry basis. The heating value of the product syngas ($\text{HHV}_{\text{syngas}}$) is simply obtained by adding the enthalpy of formation (ΔH_f) of all of the syngas species weighted on the mass fractions. It is relevant to observe that together with CO , H_2 , and CH_4 , there are light hydrocarbons as well as heavier

Table 4. Sensitivities on Syngas Molar Fractions, Mass Flow Rate, and CGE

sensitivity on equivalence ratio, $T_{g,in} = 333$ K, $STC = 0.3$			
syngas mole fractions	$\lambda = 0.15$	$\lambda = 0.176$	$\lambda = 0.20$
CO	0.207	0.226	0.211
CO ₂	0.061	0.057	0.065
H ₂	0.185	0.169	0.150
H ₂ O	0.152	0.139	0.127
N ₂	0.370	0.396	0.422
CH ₄	0.014	0.012	0.012
syngas mass flow (kg m ⁻² s ⁻¹)	0.253	0.288	0.313
cold gas efficiency (%)	80.2	93.4	92.1
sensitivity on inlet gas temperature, $\lambda = 0.176$, $STC = 0.3$			
syngas mole fractions	$T_{g,in} = 333$ K	$T_{g,in} = 373$ K	$T_{g,in} = 473$ K
CO	0.226	0.230	0.240
CO ₂	0.057	0.055	0.051
H ₂	0.169	0.170	0.172
H ₂ O	0.139	0.126	0.121
N ₂	0.396	0.395	0.391
CH ₄	0.012	0.012	0.011
syngas mass flow (kg m ⁻² s ⁻¹)	0.288	0.288	0.289
cold gas efficiency (%)	93.4	94.5	97.1
sensitivity on STC , $\lambda = 0.176$, $T_{g,in} = 333$ K			
syngas mole fractions	$STC = 0.2$	$STC = 0.3$	$STC = 0.4$
CO	0.251	0.226	0.201
CO ₂	0.040	0.057	0.071
H ₂	0.151	0.169	0.180
H ₂ O	0.114	0.139	0.147
N ₂	0.417	0.396	0.378
CH ₄	0.012	0.012	0.011
syngas mass flow (kg m ⁻² s ⁻¹)	0.277	0.288	0.297
cold gas efficiency (%)	92.1	93.4	93.5

aromatics and phenolic species (~3–4 wt % in these conditions) that are neglected in the evaluation of HHV_{syngas} .

$$HHV_{syngas} = \sum_j \omega_j \Delta H_j \quad (\text{MJ/kg}) \quad (5)$$

The equivalence ratio, i.e., the amount of air in the inlet gas, strongly affects the temperature profile, bed height, and syngas composition.

The increase of oxygen determines an increase of coal oxidation and combustion as well as gasifier temperatures. A corresponding sharp reduction of the solid residue and bed height along with a reduction of the H₂/CO ratio is also observed. Because of this high sensitivity of the gasifier performance, this parameter is only explored between 0.15 and 0.20. It is indeed quite evident that the lowest value of oxygen in the feed implies only a limited coal gasification with a large carbon content in the residual ash. Thus, the gasifier efficiency initially increases with λ , because of the completion of the gasification process, and then of course decreases, because of the successive oxidation reactions of syngas to form H₂O and CO₂. The values of the equivalence ratio adopted in this work are relatively low when compared to values of about 0.3, usually applied in gasifier units. Moreover, the residual char (see Figure 9) observed in the experimental conditions of Grieco and Baldi further confirms this low value of the equivalence ratio.

A different way to complete the gasification process, without successive oxidation reactions, is to increase the temperature of the inlet gas stream. Axial thermal profiles show a

corresponding temperature increase, and globally, an increase in the CGE is observed. In fact, the change of the inlet temperature from 333 to 473 K allows for completion of the process, because of the higher reactivity of steam gasification reactions, leading to a negligible carbon content in the solid residue.

The last operating parameter analyzed is the STC . In this case, the increase of steam partial pressure may again result in a higher steam gasification rate. The change of STC from 0.2 to 0.4 allows us to obtain a partial reduction of the carbon content in the residual ash. A significant increase of the H₂/CO ratio is also observed. In fact, CO₂ increases at the expense of CO, because of the water-gas shift reaction. For this reason, the CGE remains almost constant in these conditions.

The steam effectiveness in the endothermic gasification process requires sustainable high temperatures inside the reactor. In principle, higher values of STC allow for the increase of both the syngas flow rate and the H₂/CO ratio, with respect to higher λ values. Indeed, the optimal operating conditions of the gasifier should carefully select the proper combinations of these three parameters.

4.5. Comparisons to Experimental Data from the Sotacarbo Pilot Gasifier. Ferrara et al.⁵² analyzed the thermal decomposition of South African and Sardinian Sulcis coals and a biomass sample (pine wood chips) through thermogravimetric analysis (TGA) at different heating rates. Figure 10

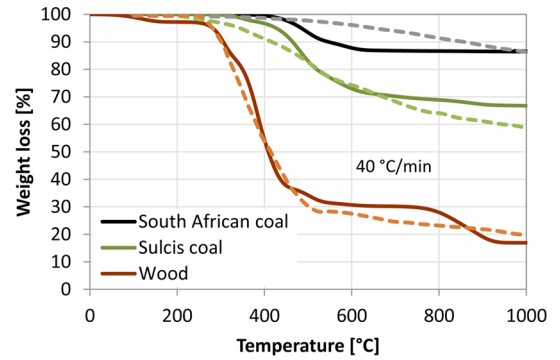


Figure 10. TGA profiles for two different coal samples and wood chips at 40 °C/min. Comparisons of experimental data (dashed lines) to model predictions (solid lines).

compares these experimental data to the predictions of the multi-step kinetic model of coal⁴¹ and biomass³³ devolatilization and clearly highlights the different behavior of the three feedstocks. Table 5 reports the proximate and ultimate analyses of two different coals and the biomass sample.

The normalized H/C/O elemental composition allows for characterization of the solid fuel as a linear combination of three reference components. Then, the devolatilization process is considered as the linear combination of the pyrolysis reactions of these three reference components. Thus, the Sulcis coal is characterized as a mixture of the three reference coals: COAL1, COAL2, and COAL3, while the South African coal also initially contains ~50% CHAR, because of the high carbon content. Similarly, the wood biomass sample is described as a combination of the three major constituents: cellulose, hemicellulose, and lignin. Again, the high C content of the pine biomass forces the feed composition toward a very high lignin content (>80%). Gas- and tar-released volatiles are in the

Table 5. Ultimate and Proximate Analyses of the Three Solid Fuels (Dry Samples)

	South African coal	Sulcis coal	wood
Ultimate Analysis (wt %)			
C	85.88	63.22	56.03
H	2.84	4.43	6.02
N	1.5	1.59	0.07
S	0.56	7.14	0.00
O	1.11	9.44	34.24
Proximate Analysis (wt %)			
fixed carbon	77.51	42.55	19.01
volatiles	14.38	43.27	78.26
moisture	0.00	0.00	2.74
ash	8.11	14.18	0.90

order of 15 and 35% for the two analyzed coals, while they are about 80% for the pine wood biomass.

The experimental data relating to the gasification of the South African bituminous coal³⁶ are used to further validate the gasifier model. These data are obtained with a significantly lower equivalence ratio and higher STC ratio, leading to a lower temperature peak, with respect to the previous analyzed conditions. Figure 11 shows the comparisons of experimental data and model predictions obtained with 10 RLs and 2 PSs.

Important deviations between calculated and experimental data are observed on both temperature profiles and product compositions. Particularly, CO and H₂ are strongly underestimated. While the peak temperature and CO₂ formation well agree with the experimental indication, the higher temperatures in the upper part of the gasifier seem to confirm a lack in the successive endothermic gasification process. These model deviations could be due to not only the assumption of negligible heat losses in the gasifier model but also the ash catalytic effect on steam gasification, which is not included in the kinetic model but possibly occurs especially with high ash contents at low temperatures.²⁰ In fact, at high temperatures, the thermal gasification reactions are already effective, covering in this way the ash catalytic effect. The next paragraph will analyze in an empirical way the possible catalytic effect of ash.

4.5.1. Model Sensitivity to the Catalytic Effect of Ash. To improve the agreement of model results and experimental data, it is necessary to analyze and empirically include the ash catalytic effect. As already mentioned, several experimental data clearly confirm their catalytic activity on steam gasification of charcoal in these operating conditions.^{37,38,40} This effect is

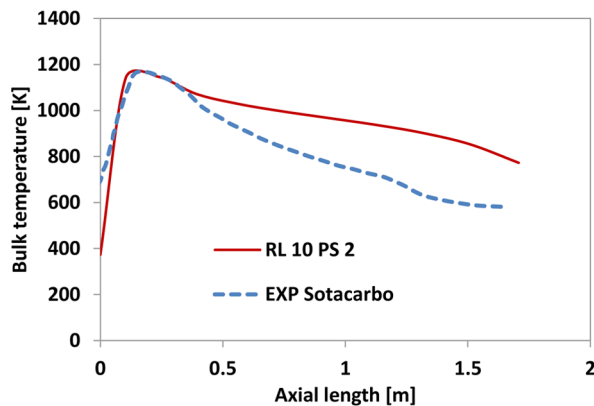


Figure 11. Comparisons of experimental data (dashed bars) of the Sotacarbo gasifier to model predictions (solid bars).

considered by simply reducing the activation energies of the steam gasification reactions of the different pseudo-components characterizing the residual char. Because of the low temperatures, the annealing effects are negligible and only CHARH and CHAR are available for the following gasification reactions:⁵³

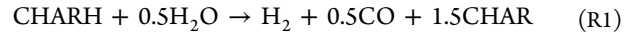


Figure 12 compares the experimental temperature profiles to the original simulation and two new simulations. The first one

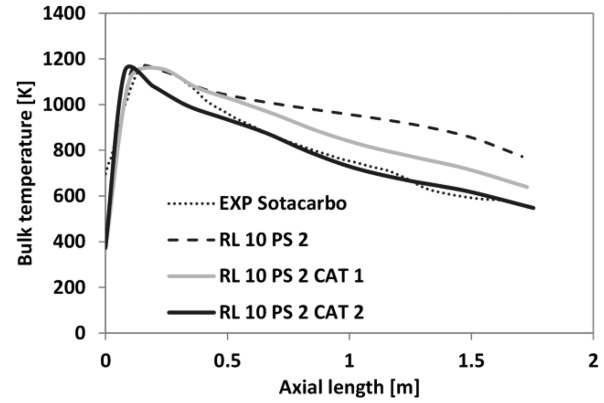


Figure 12. Catalytic effect of ash. Comparison of experimental data (dashed line) to predicted temperature profiles: original kinetic model (dotted line), model CAT 1 (gray line), and model CAT 2 (black line).

(CAT 1) is obtained by reducing the activation energy of CHARH gasification (reaction R1) by 10 kcal/mol, while the second simulation (CAT 2) was performed with a further reduction of 5 kcal/mol applied also to the CHAR gasification reaction (reaction R2). These reductions in activation energies correspond to a factor greater than 100 at gasifier temperatures of about 1000 K.

The enhancement of endothermic gasification rates reduces the temperatures above the combustion zone approaching the experimental profile. Both of the kinetic corrections are useful to improve the agreement between experimental data and model predictions.

Table 6 shows a comparison of gas-phase compositions and residual charcoal. The predicted solid residue is reduced from

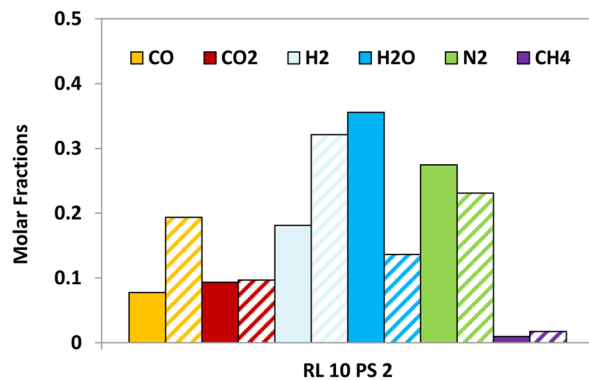


Table 6. Catalytic Effect of Ashes^a

syngas mole fractions	experimental data	original model	CAT 1 model	CAT 2 model
CO	0.1935	0.077	0.103	0.129
CO ₂	0.0968	0.093	0.090	0.091
H ₂	0.3213	0.181	0.214	0.239
H ₂ O	0.1363	0.356	0.311	0.265
N ₂	0.2311	0.275	0.264	0.260
CH ₄	0.0173	0.009	0.011	0.009
solid residue (wt %)	20.3	40.0	38.2	31.8

^aComparison of experimental and predicted syngas composition and residual char to the original model and the two modifications (CAT 1 and CAT 2).

the initial prediction from ~40 to ~30%, while the experimental data are in the range of only 20%. Also, the data of CO and H₂ would suggest the need for an additional increase of the gasification reactions. This further increase in the system reactivity would further reduce the gasifier temperatures, suggesting more critical attention toward the “average” experimental data, mainly with respect to the real achievement of the steady-state conditions.

5. CONCLUSION

A multi-scale mathematical model for the simulation of an updraft coal gasifier is discussed and analyzed in comparison to two different sets of experimental data. The novelty of this model relies on a comprehensive kinetic modeling approach, which can characterize, with reasonable detail, also the devolatilization and pyrolysis steps as well as the secondary gas-phase reactions. The best feature of the present model relies on the flexibility to handle different feedstocks, i.e., not only coal but also biomass, plastics, and RDF. A sensitivity analysis shows the strong effect of operating parameters on the quality of the produced syngas and the gasification efficiency and could provide a valuable tool to optimize them to reach the desired targets. Comparisons to experimental data show not only the model reliability but also its limits, mainly related to the catalytic effect of ash at the relatively low temperatures of the Sotacarbo gasifier. The observed deviations between model predictions and Sotacarbo experimental data first indicate the importance of including the catalytic effect of ash, meanwhile also suggesting more critical attention in properly averaging the experimental data, only after the real achievement of the steady-state conditions.

Results from the preliminary analysis described in this paper indicate that the model is suitable to support the optimization of the experimental campaigns in the Sotacarbo pilot plant, with the aim to reduce the number of experimental tests. In parallel, the new experimental results will allow for further optimization of the model.

AUTHOR INFORMATION

Corresponding Author

*Telephone: +39-0-2-2399-3273. Fax: +39-0-2-2399-3280. E-mail: flavio.manenti@polimi.it.

Notes

The authors declare no competing financial interest.

REFERENCES

- (1) Tola, V.; Pettinau, A. Power generation plants with carbon capture and storage: A techno-economic comparison between coal combustion and gasification technologies. *Appl. Energy* **2014**, *113*, 1461–1474.
- (2) Li, S.; Ji, X.; Zhang, X.; Gao, L.; Jin, H. Coal to SNG: Technical progress, modeling and system optimization through exergy analysis. *Appl. Energy* **2014**, *136*, 98–109.
- (3) Pirola, C.; Scavini, M.; Galli, F.; Vitali, S.; Comazzi, A.; Manenti, F.; Ghigna, P. Fischer–Tropsch synthesis: EXAFS study of Ru and Pt bimetallic Co based catalysts. *Fuel* **2014**, *132*, 62–70.
- (4) Ng, K. L.; Chadwick, D.; Toseland, B. A. Kinetics and modelling of dimethyl ether synthesis from synthesis gas. *Chem. Eng. Sci.* **1999**, *54* (15–16), 3587–3592.
- (5) Manenti, F.; Cieri, S.; Restelli, M.; Bozzano, G. Dynamic modeling of the methanol synthesis fixed-bed reactor. *Comput. Chem. Eng.* **2013**, *48*, 325–334.
- (6) Manenti, F.; Leon-Garzon, A. R.; Ravaghi-Ardebili, Z.; Pirola, C. Systematic staging design applied to the fixed-bed reactor series for methanol and one-step methanol/dimethyl ether synthesis. *Appl. Therm. Eng.* **2014**, *70* (2), 1228–1237.
- (7) Chen, C. J.; Hung, C. I.; Chen, W. H. Numerical investigation on performance of coal gasification under various injection patterns in an entrained flow gasifier. *Appl. Energy* **2012**, *100*, 218–228.
- (8) Manenti, F.; Cieri, S.; Restelli, M. Considerations on the steady-state modeling of methanol synthesis fixed-bed reactor. *Chem. Eng. Sci.* **2011**, *66* (2), 152–162.
- (9) Galindo, A. L.; Lora, E. S.; Andrade, R. V.; Giraldo, S. Y.; Jaen, R. L.; Cobas, V. M. Biomass gasification in a downdraft gasifier with a two-stage air supply: Effect of operating conditions on gas quality. *Biomass Bioenergy* **2014**, *61*, 236–244.
- (10) Patel, V. R.; Upadhyay, D. S.; Patel, R. N. Gasification of lignite in a fixed bed reactor: Influence of particle size on performance of downdraft gasifier. *Energy* **2014**, *78*, 323–332.
- (11) Prasad, L.; Subbarao, P. M. V.; Subrahmanyam, J. P. Pyrolysis and gasification characteristics of Pongamia residue (de-oiled cake) using thermogravimetry and downdraft gasifier. *Appl. Therm. Eng.* **2014**, *63* (1), 379–386.
- (12) Rong, L.; Maneerung, T.; Ng, J. C.; Neoh, K. G.; Bay, B. H.; Tong, Y. W.; Wang, C. H. Co-gasification of sewage sludge and woody biomass in a fixed-bed downdraft gasifier: Toxicity assessment of solid residues. *Waste Manage.* **2015**, *36*, 241–255.
- (13) Sarker, S.; Bimbela, F.; Sánchez, J. L.; Nielsen, H. K. Characterization and pilot scale fluidized bed gasification of herbaceous biomass: A case study on alfalfa pellets. *Energy Convers. Manage.* **2015**, *91*, 451–458.
- (14) Sarker, S.; Nielsen, H. K. Preliminary fixed-bed downdraft gasification of birch woodchips. *Int. J. Environ. Sci. Technol.* **2014**, 1–8.
- (15) Striugas, N.; Zakaruskas, K.; Dziugys, A.; Navakas, R.; Paulauskas, R. An evaluation of performance of automatically operated multi-fuel downdraft gasifier for energy production. *Appl. Therm. Eng.* **2014**, *73* (1), 1151–1159.
- (16) Prabowo, B.; Umeki, K.; Yan, M.; Nakamura, M. R.; Castaldi, M. J.; Yoshikawa, K. CO₂–steam mixture for direct and indirect gasification of rice straw in a downdraft gasifier: Laboratory-scale experiments and performance prediction. *Appl. Energy* **2014**, *113*, 670–679.
- (17) Emun, F.; Gadalla, M.; Majozi, T.; Boer, D. Integrated gasification combined cycle (IGCC) process simulation and optimization. *Comput. Chem. Eng.* **2010**, *34* (3), 331–338.
- (18) Dutta, P. P.; Pandey, V.; Das, A. R.; Sen, S.; Baruah, D. C. Down draft gasification modelling and experimentation of some indigenous biomass for thermal applications. *Energy Procedia* **2014**, *54*, 21–34.
- (19) Bassyouni, M.; ul Hasan, S. W.; Abdel-Aziz, M. H.; Abdelhamid, S. M. S.; Naveed, S.; Hussain, A.; Ani, F. N. Date palm waste gasification in downdraft gasifier and simulation using ASPEN HYSYS. *Energy Convers. Manage.* **2014**, *88*, 693–699.
- (20) Itai, Y.; Santos, R.; Branquinho, M.; Malico, I.; Ghesti, G. F.; Brasil, A. M. Numerical and experimental assessment of a downdraft

gasifier for electric power in Amazon using acai seed (*Euterpe oleracea* Mart.) as a fuel. *Renewable Energy* **2014**, *66*, 662–669.

(21) Keche, A. J.; Gaddale, A. P. R.; Tated, R. G. Simulation of biomass gasification in downdraft gasifier for different biomass fuels using ASPEN PLUS. *Clean Technol. Environ. Policy* **2014**, 1–9.

(22) Mendiburu, A. Z.; Carvalho, J. A.; Coronado, C. J. R. Thermochemical equilibrium modeling of biomass downdraft gasifier: Stoichiometric models. *Energy* **2014**, *66*, 189–201.

(23) Mendiburu, A. Z.; Carvalho, J. A.; Zanzi, R.; Coronado, C. R.; Silveira, J. L. Thermochemical equilibrium modeling of a biomass downdraft gasifier: Constrained and unconstrained non-stoichiometric models. *Energy* **2014**, *71*, 624–637.

(24) Mendiburu, A. Z.; Roberts, J. J.; Carvalho, J. A.; Silveira, J. L. Thermodynamic analysis and comparison of downdraft gasifiers integrated with gas turbine, spark and compression ignition engines for distributed power generation. *Appl. Therm. Eng.* **2014**, *66* (1–2), 290–297.

(25) He, T.; Han, D.; Wu, J.; Li, J.; Wang, Z.; Wu, J. Simulation of biomass gasification and application in pilot plant. *Energy Technol.* **2015**, *3* (2), 162–167.

(26) Tapasvi, D.; Kempegowda, R. S.; Tran, K. Q.; Skreiberg, Ø.; Grønli, M. A simulation study on the torrefied biomass gasification. *Energy Convers. Manage.* **2015**, *90*, 446–457.

(27) Soltani, S.; Athari, H.; Rosen, M. A.; Mahmoudi, S. M. S.; Morosuk, T. Thermodynamic analyses of biomass gasification integrated externally fired, post-firing and dual-fuel combined cycles. *Sustainability* **2015**, *7* (2), 1248–1262.

(28) Puig-Arnavat, M.; C, B. J.; A, C. Review and analysis of biomass gasification models. *Renewable Sustainable Energy Rev.* **2010**, *14*, 2841–2851.

(29) Ismail, T. M.; El-Salam, M. A. Numerical and experimental studies on updraft gasifier HTAG. *Renewable Energy* **2015**, *78*, 484–497.

(30) Vascellari, M.; Roberts, D. G.; Harris, D. J.; Hasse, C. From laboratory-scale experiments to industrial-scale CFD simulations of entrained flow coal gasification. *Fuel* **2015**, *152*, 58–73.

(31) Zhong, H.; Lan, X.; Gao, J. Numerical simulation of pitch-water slurry gasification in both downdraft single-nozzle and opposed multi-nozzle entrained-flow gasifiers: A comparative study. *J. Ind. Eng. Chem.* **2015**, DOI: 10.1016/j.jiec.2014.12.033.

(32) Masmoudi, M. A.; Sahraoui, M.; Grioui, N.; Halouani, K. 2-D modeling of thermo-kinetics coupled with heat and mass transfer in the reduction zone of a fixed bed downdraft biomass gasifier. *Renewable Energy* **2014**, *66*, 288–298.

(33) Corbetta, M.; Frassoldati, A.; Bennadji, H.; Smith, K.; Serapiglia, M. J.; Gauthier, G.; Melkior, T.; Ranzi, E.; Fisher, E. M. Pyrolysis of centimeter-scale woody biomass particles: Kinetic modeling and experimental validation. *Energy Fuels* **2014**, *28* (6), 3884–3898.

(34) Ranzi, E.; Pierucci, S.; Aliprandi, P. C.; Stringa, S. Comprehensive and detailed kinetic model of a traveling grate combustor of biomass. *Energy Fuels* **2011**, *25* (9), 4195–4205.

(35) Grieco, E. M.; Baldi, G. Predictive model for countercurrent coal gasifiers. *Chem. Eng. Sci.* **2011**, *66*, 5749–5761.

(36) Pettinau, A.; Orsini, A.; Cali, G.; Ferrara, F. The Sotacarbo coal gasification experimental plant for a CO₂-free hydrogen production. *Int. J. Hydrogen Energy* **2010**, *35* (18), 9836–9844.

(37) Timpe, R. C.; Kulas, R. W.; Hauserman, W. B. Catalytic effect on the gasification of a bituminous Argonne premium coal sample using wood ash or taconite as additive. *Prepr. Pap.—Am. Chem. Soc., Div. Fuel Chem.* **1991**, *36* (3), 892–897.

(38) Otto, K.; Bartosiewicz, L.; Shelef, M. Catalysis of carbon-steam gasification by ash components from two lignites. *Fuel* **1979**, *58* (2), 85–91.

(39) Köpsel, R.; Zabawski, H. Catalytic effects of ash components in low rank coal gasification: 1. Gasification with carbon dioxide. *Fuel* **1990**, *69* (3), 275–281.

(40) Köpsel, R.; Zabawski, H. Catalytic effects of ash components in low rank coal gasification: 2. Gasification with steam. *Fuel* **1990**, *69* (3), 282–288.

(41) Sommariva, S.; Grana, R.; Maffei, T.; Pierucci, S.; Ranzi, E. A kinetic approach to the mathematical model of fixed bed gasifiers. *Comput. Chem. Eng.* **2011**, *35*, 928–935.

(42) Maffei, T.; Senneca, O.; Ranzi, E.; Salatino, P. Pyrolysis, annealing and char combustion/oxy-combustion for CFD codes. *XXXIV Meeting of the Italian Section of the Combustion Institute*; Rome, Italy, Oct 24–26, 2011.

(43) Ranzi, E.; Frassoldati, A.; Grana, R.; Cuoci, A.; Faravelli, T.; Kelley, A. P.; Law, C. K. Hierarchical and comparative kinetic modeling of laminar flame speeds of hydrocarbon and oxygenated fuels. *Prog. Energy Combust. Sci.* **2012**, *38* (4), 468–501.

(44) Ranzi, E.; Corbetta, M.; Manenti, F.; Pierucci, S. Kinetic modeling of the thermal degradation and combustion of biomass. *Chem. Eng. Sci.* **2014**, *110*, 2–12.

(45) Mettler, M. S.; Vlachos, D. G.; Dauenhauer, P. J. Top ten fundamental challenges of biomass pyrolysis for biofuels. *Energy Environ. Sci.* **2012**, *5*, 7797–7809.

(46) Buzzi-Ferraris, G.; Manenti, F. BzzMath: Library overview and recent advances in numerical methods. *Comput.-Aided Chem. Eng.* **2012**, *30*, 1312–1316.

(47) Manenti, F.; Dones, I.; Buzzi-Ferraris, G.; Preisig, H. A. Efficient numerical solver for partially structured differential and algebraic equation systems. *Ind. Eng. Chem. Res.* **2009**, *48* (22), 9979–9984.

(48) Ranzi, E.; Cuoci, A.; Faravelli, T.; Frassoldati, A.; Migliavacca, G.; Pierucci, S.; Sommariva, S. Chemical kinetics of biomass pyrolysis. *Energy Fuels* **2008**, *22* (6), 4292–4300.

(49) Stark, A. K.; Bates, R. B.; Zhao, Z.; Ghoniem, A. F. Prediction and validation of major gas and tar species from a reactor network model of air-blown fluidized bed biomass gasification. *Energy Fuels* **2015**, *29* (4), 2437–2452.

(50) Basu, P. *Biomass Gasification and Pyrolysis*; Academic Press: Waltham, MA, 2010.

(51) Institute of Gas Technology (IGT). *Coal Conversion Systems Technical Data Book*; National Technical Information Service (NTIS): Springfield, VA, 1978; ERDA FE-2286-32.

(52) Ferrara, F.; Orsini, A.; Plaisant, A.; Pettinau, A. Pyrolysis of coal, biomass and their blends: Performance assessment by thermogravimetric analysis. *Bioresour. Technol.* **2014**, *171*, 433–441.

(53) Maffei, T.; Frassoldati, A.; Cuoci, A.; Ranzi, E.; Faravelli, T. Predictive one step kinetic model of coal pyrolysis for CFD applications. *Proc. Combust. Inst.* **2013**, *34* (2), 2401–2410.

(54) Maffei, T.; Sommariva, S.; Ranzi, E.; Faravelli, T. A predictive kinetic model of sulfur release from coal. *Fuel* **2012**, *91* (1), 213–223.

(55) Maffei, T.; Khatami, R.; Pierucci, S.; Faravelli, T.; Ranzi, E.; Levendis, Y. A. Experimental and modeling study of single coal particle combustion in O₂/N₂ and oxy-fuel (O₂/CO₂) atmospheres. *Combust. Flame* **2013**, *160* (11), 2559–2572.